Biochemical and Biophysical Research Communications 436 (2013) 551–556

Contents lists available at SciVerse ScienceDirect

Biochemical and Biophysical Research Communications

journal homepage: www.elsevier.com/locate/ybbrc

Characterization of the biochemical and biophysical properties of the *Saccharomyces cerevisiae* phosphate transporter Pho89

Palanivelu Sengottaiyan [a,1], Jitka Petrlova [b], Jens O. Lagerstedt [b], Lorena Ruiz-Pavon [a], Madhu S. Budamagunta [c], John C. Voss [c], Bengt L. Persson [a,*]

[a] Linnaeus University Centre for Biomaterials Chemistry, Department of Chemistry and Biomedical Sciences, Linnaeus University, SE-391 82 Kalmar, Sweden
[b] Department of Experimental Medical Science, Lund University, SE-221 84 Lund, Sweden
[c] Department of Biochemistry and Molecular Medicine, University of California, Davis, CA 95616, USA

ARTICLE INFO

Article history:
Received 3 June 2013
Available online 12 June 2013

Keywords:
Pho89
Pichia pastoris
Oligomer
Reconstitution
Phosphate transport
Circular dichroism

ABSTRACT

In *Saccharomyces cerevisiae*, Pho89 mediates a cation-dependent transport of Pi across the plasma membrane. This integral membrane protein belongs to the Inorganic Phosphate Transporter (PiT) family, a group that includes the mammalian Na^+/Pi cotransporters Pit1 and Pit2. Here we report that the *Pichia pastoris* expressed recombinant Pho89 was purified in the presence of Foscholine-12 and functionally reconstituted into proteoliposomes with a similar substrate specificity as observed in an intact cell system. The alpha-helical content of the Pho89 protein was estimated to 44%. EPR analysis showed that purified Pho89 protein undergoes conformational change upon addition of substrate.

1. Introduction

The *Saccharomyces cerevisiae* Pho89 is an integral plasma membrane protein of 574 amino acids that belongs to the Inorganic Phosphate Transporter (PiT) family (Transport Classification Database (TCDB) Number 2.A.20) [1,2]. Whole genome analysis of gene expression revealed that the *PHO89* expression is induced by different stress conditions, such as Pi starvation, alkaline pH, Mg^{2+} starvation, Ca^{2+} stress and cell wall damage [3–5]. Pho89 is vital for maintenance of Pi homeostasis under stress conditions [3] and mediates the coupled translocation of Pi and Na^+ across the membrane, using the energy of the inwardly directed Na^+ gradient (ΔpNa^+) [6].

Pho89 shares significant amino acid identity with the PiT family members, which include the mammalian type III Na^+/Pi cotransporters Pit1 and Pit2 [7], the plant *Arabidopsis thaliana* Pht2 protein [8] and the *Neurospora crassa* Pho4 protein [9]. Membrane topology analyses have suggested that the Pho89 protein consists of 12 transmembrane domains (TMDs), with both N- and C-termini located at the periplasmic side, and a large intracellular hydrophilic loop positioned between the seventh and eighth TMDs [10–12]. Recently, functional studies have shown that glutamic acid residues at position 55 and 491 of Pho89, both located in the transmembrane regions and conserved in all PiT family members, are essential for Pi transport activity [10,13]. Moreover, members of the PiT family have been shown to form oligomers at the cell surface that may be essential for their functions [14,15]. Biochemical and genetic studies have revealed that the impaired human Pit2 transporter is functionally associated with hyperphosphatemia-induced calcification of vascular tissue and familial idiopathic basal ganglia calcification [16,17].

Detailed information about the molecular mechanism and regulation of Pho89 is lacking. We have previously shown that purified recombinant Pho89 protein produced in *Pichia pastoris* retain the oligomeric state when treated with different detergents [14]. Furthermore, the Pho89 protein purified in the presence of Triton X-100 was functionally reconstituted into proteoliposomes and exhibited Na^+-dependent Pi transport activity driven by an inward-directed Na^+ gradient (ΔpNa^+) [14]. In order to correlate the function of the Pho89 transporter with the protein structure, we have in this study utilized biochemical and biophysical meth-

Abbreviations: CD, circular dichroism; ΔpNa^+, electrochemical Na^+ concentration gradient; EPR, electron paramagnetic resonance.

* Corresponding author. Fax: +46 480 446262.
E-mail address: bengt.persson@lnu.se (B.L. Persson).

[1] Present address: Institute of Life Sciences, Université Catholique de Louvain, BE-1348 Louvain-la-Neuve, Belgium.

0006-291X
http://dx.doi.org/10.1016/j.bbrc.2013.06.011

ods to gain further knowledge on the structure/function relationship of the protein.

2. Materials and methods

The nitroxide spin label, MTSL (2,2,5,5-tetramethylpyrrolin-3-methanethiosulfonate spin label) was obtained from Toronto Research Chemicals (Canada). [^{32}P]-orthophosphate (carrier-free) was purchased from Perkin Elmer (Waltham, MA, USA). Foscholine-12 was obtained from Anatrace (Maumee, OH, USA). Complete EDTA-free protease inhibitor cocktail tablet was from Roche Diagnostics (Basel, Switzerland). The lipids and Bio-Beads (SM-2) were obtained from Avanti Polar lipids (Redhill, Surrey, UK) and Bio-Rad (Hercules, CA, USA), respectively. His-Trap chelating column was from GE Healthcare (Pittsburgh, PA, USA). The HRP-conjugated mAb against Myc was obtained from Invitrogen (Carlsbad, CA, USA).

2.1. Purification of recombinant Pho89

The full-length *S. cerevisiae* high-affinity PiT Pho89 was expressed in *P. pastoris* and purified by affinity chromatography followed by gel filtration chromatography essentially as described [14]. The complete procedure is provided in Supplementary text (S.1.1). The purity of the recombinant Pho89 protein was estimated by analysis of aliquots of purified Pho89 protein separated on a 10% SDS–polyacrylamide gel stained with Coomassie brilliant blue R-250. The fractions corresponding to the Pho89 protein were identified by Western blot using anti-myc-HRP antibody. The Pho89 protein enriched fractions were pooled and used for further analysis either by functional or biophysical studies.

2.2. Spin labeling of purified Pho89

The Pho89 protein enriched fractions were pooled, and spin-labeling was performed as described previously [18]. In brief, the spin-labeling of the Pho89 protein was carried out while the protein was bound to a His-Trap Ni^{2+} affinity column (GE Healthcare, USA) previously equilibrated with the spin-labeling buffer (50 mM Tris/HCl, pH 8.0, 100 mM NaCl, 10% glycerol, 30 mM imidazole and 0.1% Foscholine-12). Subsequently, the spin-labeling buffer containing 300 μM (1-oxyl-2,2,5,5-tetramethylpyrroline-3-methyl) methanethiosulfonate spin label was applied onto the column and left at room temperature for 30 min. The unbound spin label was washed out with the spin-labeling buffer after which the bound spin-labeled Pho89 protein was eluted from the column with buffer containing 1 M imidazole.

2.3. Transport measurements with proteoliposomes

The purified Pho89 protein was incorporated into liposomes via a reconstitution method described previously [19,20]. The detailed procedure is provided in Supplementary text (S.1.2). Phosphate uptake was measured in proteoliposomes containing Pho89 protein. Aliquots of 2 μl of the proteoliposomes were diluted 25-fold in 25 mM Tris/succinate, pH 10, containing 0.11 mM of [^{32}P] orthophosphate (carrier-free, 50 mCi/mmol; 1 mCi = 37 MBq; Perkin Elmer, USA) in the absence or presence of 50 mM NaCl, 50 mM KCl or 50 mM LiCl to create an artificial ion gradient. The suspension was incubated at room temperature for 10 min. Pi transport was terminated by the addition of 1 ml of ice-cold assay buffer, followed by rapid filtration (using the filter type Supor-200, 0.2 μm; Gelman Sciences, Ann Arbor, MI, USA) [19,20] under vacuum and three washes with the same ice-cold buffer after which the radioactivity retained on the filter was determined by liquid scintillation spectrometry. Where indicated, the uptake experiments were carried out using 100 μM ^{32}P in competition with 2.5 mM nonlabeled effectors (phosphate, methylphosphonate, dimethylphosphonate, trimethylphosphonate, phosphoacetic acid and phosphocholine).

2.4. Circular dichroism spectroscopy

Circular dichroism (CD) measurements of the Pho89 protein (0.035 mg/ml) in 50 mM Tris/HCl, pH 8.0, 200 mM NaCl, 10% glycerol, 1 mM PMSF and 0.1% Foscholine-12 were performed on a Jasco J-810 spectropolarimeter equipped with a Jasco CDF-426S Peltier set to 25 °C as previously described [21]. In short, solubilized Pho89 protein was placed in a 0.1 mm quartz cuvette and, after extensive purging with nitrogen, scanned in the region 200–260 nm (scan speed was 20 nm/min). Averages of five scans were baseline-subtracted (50 mM Tris/HCl, pH 8.0, 200 mM NaCl, 10% glycerol, 1 mM PMSF and 0.1% Foscholine-12) and the alpha-helical content was calculated from the molar ellipticity at 222 nm from three independent analyses as previously described [22]. For thermal stability experiments, spectra were obtained from heating of Pho89 protein at the temperature range from 10 °C to 80 °C with 2.5 °C increments. The Boltzmann function within the GraphPad software (GraphPad Software, Inc., CA, USA) was used to fit the molar ellipticity values at 222 nm of the temperature gradient to a sigmoidal fit curve.

2.5. Mass-spectrometry analysis

Mass spectrometry (MS) analysis was performed at the core facility Swegene Centre for Integrative Biology at Lund University (SCIBLU). A band of purified Pho89 was cut from the 10% SDS–PAGE gel after Coomassie staining. This sample was provided to SCIBLU for further analysis by MALDI MS/MS analysis of trypsin-digested protein, and database search. The results confirmed the identification of purified Pho89 protein and supported the result from Western blot analysis.

2.6. Electron Paramagnetic Resonance (EPR) of purified Pho89

EPR measurements were carried out in a JEOL X-band spectrometer fitted with a loop-gap resonator. Aliquots (5 μl) of purified spin-labeled Pho89 protein (1 mg/ml) were placed in sealed quartz capillaries and loaded in the resonator. Spectra were acquired at room temperature (20–22 °C) from a single 2 min scan over a field of 100 G at a microwave power of 2 mW and a modulation amplitude optimized to the natural line width of the individual spectrum (0.5–1.5 G). Spectra were obtained in the presence and absence of 1 mM NaCl (in buffer composed of 50 mM Tris/HCl, pH 8.0, 10% glycerol and 0.1% Foscholine-12).

3. Results and discussion

3.1. Functional characterization of purified recombinant Pho89 with Foscholine-12

In order to characterize the biochemical and biophysical properties of the protein, Pho89 was recombinantly expressed in *P. pastoris*, solubilized and purified with Foscholine-12, a zwitterionic phospholipid-like detergent that provides a suitable membrane-like environment and has been successfully used for structural studies of other membrane proteins [23–25]. The homogeneity of purified Pho89 protein was evaluated by SDS–PAGE analysis (Fig. 1A) [14]. We next assessed whether the Foscholine-12 purified recombinant Pho89 was functional by reconstitution into liposomes via a reconstitution procedure previously established for

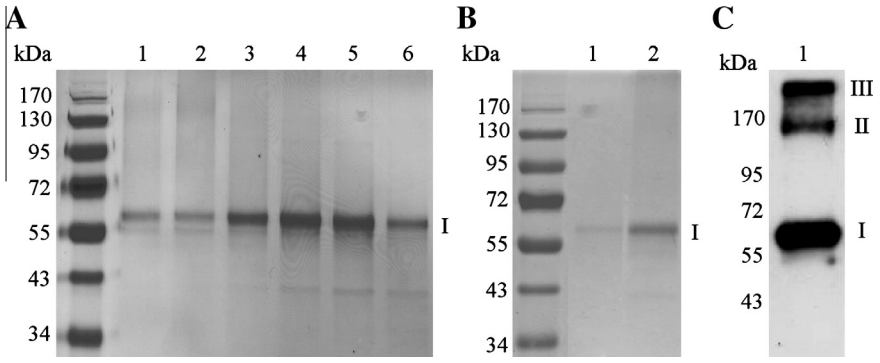

Fig. 1. Purification and reconstitution of recombinant Pho89 protein. Isolated membranes from *P. pastoris* expressing recombinant Pho89 protein was solubilized in Foscholine-12 and purified by Ni^{2+} affinity chromatography followed by gel-filtration chromatography. (A) Aliquots of purified Pho89 protein from gel-filtration fractions (lanes 1–6) were separated by 10% SDS–PAGE followed by Coomassie Blue staining. (B) Pooled gel-filtration fractions containing Pho89 protein (lane 1) were reconstituted into liposomes as described in Section 2. The presence of purified Pho89 in proteoliposomes (lane 2) was detected by 10% SDS–PAGE followed by Coomassie Blue staining. (C) Pho89 contained in proteoliposomes were detected by Western blotting with HRP-conjugated antibody against Myc. The positions of monomeric (I), dimeric (II) and oligomeric (III) species of Pho89 are indicated. All samples were treated with 2× urea loading sample buffer at 37 °C for 30 min before analysis.

Pi transporters [14,19,20] followed by Pi uptake measurements. The incorporation of purified recombinant Pho89 into liposomes was verified by SDS–PAGE (Fig. 1B) followed by Western-blot analysis which revealed that the protein appeared as bands of about 63, 140 and 520 kDa, corresponding to the monomeric, dimeric and oligomeric masses of the protein, respectively (Fig. 1C). This result indicated that the Pho89 protein was present as the oligomeric form both in the detergent solution [14] and, presumably, also in the lipid bilayer (Fig. 1C). Also, mass spectrometry analysis confirmed the identification of the Pho89 protein.

As reported previously, the Pho89 has an alkaline pH optimum (pH 9.5) and utilizes the Na^+ gradient (ΔpNa^+) as a driving force to transport Pi across the cell membrane. An inward-directed sodium gradient was established by diluting proteoliposomes into the assay mixture containing 50 mM NaCl. As shown in Fig. 2A, the level of ^{32}P accumulation was markedly stimulated (10–12 fold) in the presence of Na^+, whereas no significant uptake could be observed in the absence of Na^+. Under similar conditions, the substrate specificity of Pho89 was also investigated. We found that proteoliposomes containing Pho89 retained the same substrate specificity as observed in intact cell system [12,26]. These results suggested that Pho89 preferred Na^+ as a co-solute followed by K^+ and Li^+, to drive Pi uptake similar to the situation with the Pho4 transporter of *N. crassa* [9] and the melibiose permease of *E. coli* [27]. So far, Pho89 is the only protein reported as Na^+-Pi transporter in the group of alkali metal cation transporters in *S. cerevisiae* suggesting its importance as a specific Na^+-dependent phosphate transporter [28].

To investigate whether the Pho89 protein specifically transports Pi and/or also binds other anions in a competitive manner, we measured the effect of various non-labeled effectors on the Pi uptake in the proteoliposomes containing the Pho89 protein and in control liposomes (Fig. 2B). The most efficient competitors were non-labeled Pi and its analogues, phosphonoacetic acid, methylphosphonate, followed by dimethylphosphonate (Fig. 2C). Replacement of a hydroxyl group by a methyl group in methylphosphonate reduced the uptake levels of ^{32}P by about 85%. The additional methyl group in dimethylphosphonate affected the uptake to a similar extent (83% less uptake of ^{32}P), indicating that the binding site is able to accommodate both of these analogues. Different to methylphosphonate and dimethylphosphonate, the analogue trimethylphosphonate had very low impact on the transport activity. In contrast, when the same transport assays using the analogue methylphosphonate were carried out with the H^+-coupled Pho84 phosphate transporter in earlier analyses it was shown that methylphosphonate is not efficiently recognized as a substrate, but instead affects trafficking of Pho84 in *S. cerevisiae* [29].

The addition of a carboxylic acid group to phosphate in phosphonoacetic acid (PAA) reduced the Pho89 mediated uptake by about 90%. Previously, it was demonstrated that PAA also acts as a competitive inhibitor of Pho84 mediated phosphate transport suggesting direct binding to the phosphate-binding site of Pho84 in a similar way as phosphate [30]. The addition of a choline group in phosphocholine was found to be the least efficient competitor, showing no substantial influence on the Pho89 catalyzed Pi uptake.

3.2. Circular dichroism spectroscopy

We used circular dichroism (CD) spectroscopy to estimate the secondary structure content of the purified Pho89 protein in solution (25 °C; 50 mM Tris/HCl, pH 8.0, 200 mM NaCl, 10% glycerol, 1 mM PMSF and 0.1% Foscholine-12). The conditions mimicked those previously used for estimating the helical content in the human Na^+/H^+ exchanger NheI [24]. The shape of the obtained spectra (Fig. 3A) indicates a significant proportion of alpha-helical structure [31] of the purified Pho89 protein (Fig. 3A). Based on calculations from the background-subtracted molar ellipticity value at 222 nm the alpha-helical content of the Pho89 protein is estimated to 44.4 ± 1.4% (SEM; $n = 3$), which corresponds to about 254 amino acid residues of the total 574 residues of the Pho89 protein. Hydropathy and homology analyses suggest 12 transmembrane regions [10,11] and given 15–20 residues per transmembrane helix the apparent alpha helical content fits well with the expected content (i.e., >180 residues in alpha-helical structure).

Next, CD spectroscopy was used to analyze the thermal stability of the Pho89 protein (Fig. 3B). A loss of alpha helical secondary structure was observed with increasing temperature as shown by a change in the molar ellipticity value at 222 nm. The Boltzmann function within the GraphPad software was used to fit the molar ellipticity values at 222 nm of the temperature gradient to a sigmoidal fit curve and to calculate the melting temperature (T_m) of the Pho89 protein. Unfolding caused by step-wise increase of temperature (2.5 °C increments) resulted in sigmoidal, monophasic transition with an apparent T_m 41.6 ± 3.0 °C (SEM; $n = 3$). We also examined the potential use of CD spectroscopy to investigate the Pho89 protein in proteoliposomes. Due to the relatively low protein concentration in relation to high absorbance by the phospholipids in the proteoliposomes we were unable to determine the secondary structure of reconstituted Pho89 protein. However, the thermal stability of the transporter combined with an apparent ordered structure of the detergent-solubilized Pho89 protein sup-

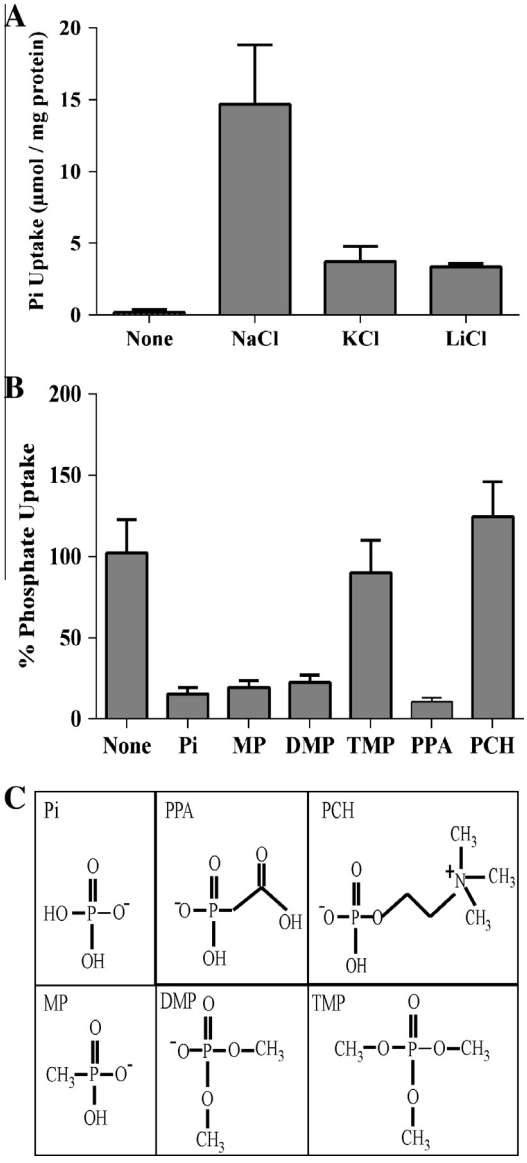

Fig. 2. Substrate specificity characteristics of proteoliposomes containing purified recombinant Pho89. (A) The reconstituted proteoliposomes were preloaded with 25 mM K^+-HEPES buffer at pH 7.0, and diluted 25-fold in assay buffer (25 mM Tris–succinate, pH 10) in the absence or presence 50 mM NaCl, KCl or LiCl. Transport was initiated by addition of 100 µM [^{32}P]. The Pi transport was assayed as described in Section 2 after 10 min incubation. (B) Effect of phosphate analogues on phosphate transport. Uptake was carried out under the same conditions as in (A), but in the absence (None) or presence of 2.5 mM nonlabeled effectors, phosphate (Pi), methyl phosphonate (MP), di-methyl phosphonate (DMP), trimethyl phosphonate (TMP), phosphonoacetic acid (PPA) and phosphocholine (PCH) which were added 2 min before [^{32}P] and stopped by rapid filtration. (C) Schematic representation of the chemical structures of different analogs used in graph (B). Data represents the mean ± S.D. of three independent experiments with four replicates each.

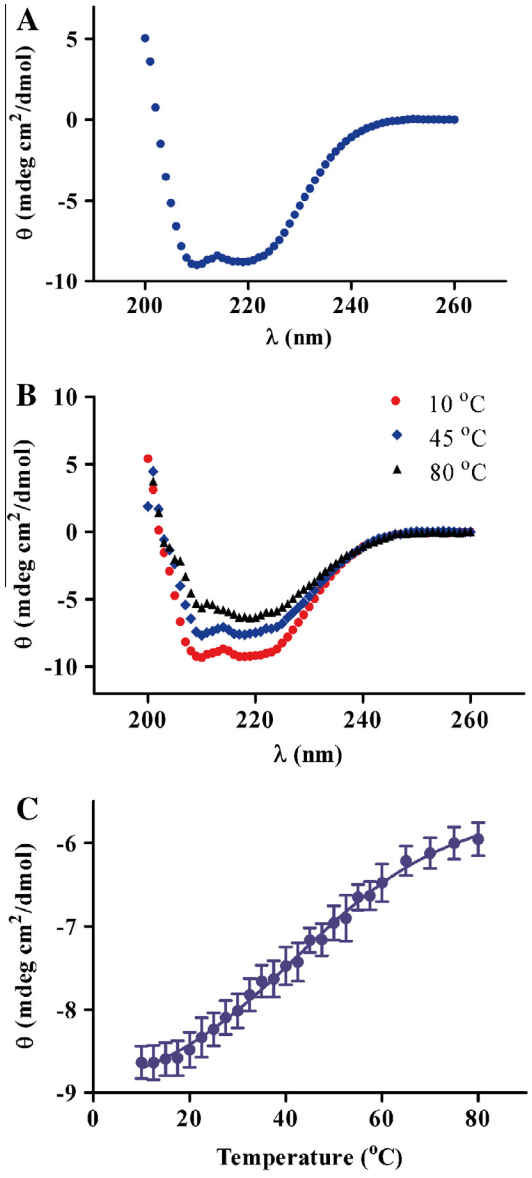

Fig. 3. Secondary structure of recombinant Pho89 was determined by CD spectroscopy. (A) Recombinant Pho89 protein (0.035 mg/ml) was placed in a 0.1 mm quartz cuvette and scanned at 25 °C in the region 200–260 nm with a scan speed of 20 nm/min. The molar ellipticity at 222 nm from three independent experiments was used to calculate the alpha-helical content. (B) Thermal unfolding of recombinant Pho89 was monitored by changes in CD spectra. CD spectra of Pho89 protein obtained at temperatures 10, 45 and 80 °C are shown. (C) Thermal stability of Pho89 was determined by changes in molar ellipticity at 222 nm at 2.5 °C increments in the temperature range between 10 and 80 °C. A T_m of 41.6 ± 3.0 °C (SEM; $n = 3$) was determined by fitting of the Boltzmann function, which was used to fit the molar ellipticity values at 222 nm of the temperature gradient to a sigmoidal fit curve. All CD analysis of Pho89 (0.035 mg/ml) was measured in 50 mM Tris/HCl, pH 8.0, 200 mM NaCl, 10% glycerol, 1 mM PMSF and 0.1% Foscholine-12.

ports the notion that this structure arrangement likely resembles that of Pho89 protein embedded in a phospholipid bilayer.

3.3. EPR spectroscopy analysis

EPR spectroscopy was used to assess the integrity of the protein and also to investigate the potential influence of the structure by the presence of substrate. To do this, the free –SH groups of the native five Cys residues in Pho89 were reacted with the thiol-specific spin label, MTSL [32,33]. The Pho89 structure contains five native cysteines, of which two are expected to be directly accessible in extra-membrane regions [10,11], although in most cases MTSL reacts rapidly with free –SH groups at interior sites as well. An obvious limitation of the analysis is thus the lack of information on the number and exact position of the labeled cysteine(s). However, the data from the native Cys residues can be informative on the relative order of the recombinant protein molecule, as the EPR spectrum of the attached nitroxide is highly sensitive to the rapid backbone motions of unfolded proteins or disordered protein regions [18,34]. The spectrum of Pho89 purified in Foscholine-12, spin labeled with

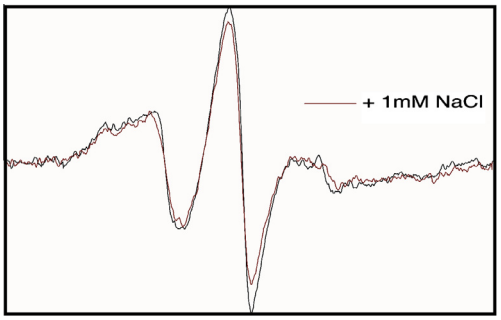

Fig. 4. EPR analysis of Pho89 reacted with the MTSL nitroxide spin label. Shown are spectra of purified Pho89 in Foscholine-12 detergent obtained in the absence (black trace) and presence (red trace) of 1 mM Na^+. Each spectrum represents the identical number of spins present in ~1 mg/ml protein.

MTSL, and scanned by EPR spectroscopy is shown in Fig. 4. Notably, there is an absence of weakly immobilized signal, suggesting each of the spin labels is attached to an ordered backbone. This finding is consistent with the CD results, in that regular secondary structure is abundant when the Pho89 protein is solubilized in Foscholine-12 detergent micelles. As shown in Fig. S1, the CD spectra of Pho89 with attached spin label, are identical to the Pho89 without attached spin label. These results demonstrate the spin label does not introduce major changes to the secondary structure of the protein, which would be expected if the Cys modification resulted in the mis-folding of the protein.

The relatively broad EPR spectrum obtained from the spin labeled Pho89 suggests multiple correlation times contribute to the modulation of the hyperfine anisotropy, each with rates of motion longer than 1 ns [35]. To explore whether the dynamics of one or more attached spin labels were altered upon ligand binding, we also analyzed purified Pho89 by EPR after addition of NaCl (final concentration 1 mM). As evident in Fig. 4, addition of NaCl results in a slight broadening of the EPR spectrum. The most likely explanation for this result is a decrease in the conformational entropy in the protein upon substrate binding, which slows the reorientation of one or more spin probes. Thus, in isolation, at least one of the spin labeled positions should function as an effective marker for Na^+ ligand binding and perhaps a kinetic state.

In conclusion, we have shown that full-length *S. cerevisiae* high-affinity PiT Pho89, solubilized and purified in the presence of Foscholine-12, has retained oligomer formation and exhibit Na^+-driven Pi cotransport activity when reconstituted in proteoliposomes, and that this Pi uptake can be inhibited by phosphate analogues in a structurally size-dependent manner. Moreover, CD analysis showed that the α-helical content of the Pho89 protein corresponds to that expected for a membrane protein composed of 12 transmembrane helices. Finally, EPR spectroscopy reveal structural conformational change upon substrate binding to the Pho89 protein. The findings of the present study could be useful to gain mechanistic insights into the biological functions and regulations of Pho89 transporter and also open the way for biophysical and structural studies of PiT family members.

Acknowledgments

This work was supported by a research grant to B.L.P. from the Swedish Research Council (621-2007-6144), and research grants to J.O.L. from the Swedish Research Council (522-2008-3724, 7480) and the Crafoord Foundation. J.P. and J.O.L. acknowledge support from the Wenner-Gren Foundation.

Appendix A. Supplementary data

Supplementary data associated with this article can be found, in the online version, at http://dx.doi.org/10.1016/j.bbrc.2013.06.011.

References

[1] M.H. Saier Jr., A functional-phylogenetic classification system for transmembrane solute transporters, Microbiol. Mol. Biol. Rev. 64 (2000) 354–411.
[2] I.C. Forster, N. Hernando, J. Biber, H. Murer, Phosphate transport kinetics and structure–function relationships of SLC34 and SLC20 proteins, Curr. Top. Membr. 70 (2012) 313–356.
[3] J. Pattison-Granberg, B.L. Persson, Regulation of cation-coupled high-affinity phosphate uptake in the yeast *Saccharomyces cerevisiae*, J. Bacteriol. 182 (2000) 5017–5019.
[4] R. Serrano, A. Ruiz, D. Bernal, J.R. Chambers, J. Arino, The transcriptional response to alkaline pH in *Saccharomyces cerevisiae*: evidence for calcium-mediated signalling, Mol. Microbiol. 46 (2002) 1319–1333.
[5] G. Wiesenberger, K. Steinleitner, R. Malli, W.F. Graier, J. Vormann, R.J. Schweyen, J.A. Stadler, Mg2+ deprivation elicits rapid Ca2+ uptake and activates Ca2+/calcineurin signaling in *Saccharomyces cerevisiae*, Eukaryot. Cell 6 (2007) 592–599.
[6] G.M. Roomans, F. Blasco, G.W. Borst-Pauwels, Cotransport of phosphate and sodium by yeast, Biochim. Biophys. Acta 467 (1977) 65–71.
[7] M.P. Kavanaugh, D. Kabat, Identification and characterization of a widely expressed phosphate transporter/retrovirus receptor family, Kidney Int. 49 (1996) 959–963.
[8] P. Daram, S. Brunner, C. Rausch, C. Steiner, N. Amrhein, M. Bucher, Pht2;1 encodes a low-affinity phosphate transporter from Arabidopsis, Plant Cell 11 (1999) 2153–2166.
[9] W.K. Versaw, R.L. Metzenberg, Repressible cation-phosphate symporters in *Neurospora crassa*, Proc. Natl. Acad. Sci. USA 92 (1995) 3884–3887.
[10] M.R. Andersson, D.R. Samyn, B.L. Persson, Mutational analysis of conserved glutamic acids of Pho89, a *Saccharomyces cerevisiae* high-affinity inorganic phosphate:Na+ symporter, Biologia 67 (2012) 1056–1061.
[11] B.L. Persson, J. Petersson, U. Fristedt, R. Weinander, A. Berhe, J. Pattison, Phosphate permeases of *Saccharomyces cerevisiae*: structure, function and regulation, Biochim. Biophys. Acta 1422 (1999) 255–272.
[12] P. Martinez, B.L. Persson, Identification, cloning and characterization of a derepressible Na+-coupled phosphate transporter in *Saccharomyces cerevisiae*, Mol. Gen. Genet. 258 (1998) 628–638.
[13] P. Bottger, L. Pedersen, Two highly conserved glutamate residues critical for type III sodium-dependent phosphate transport revealed by uncoupling transport function from retroviral receptor function, J. Biol. Chem. 277 (2002) 42741–42747.
[14] P. Sengottaiyan, L. Ruiz-Pavon, B.L. Persson, Functional expression, purification and reconstitution of the recombinant phosphate transporter Pho89 of *Saccharomyces cerevisiae*, FEBS J. 280 (2013) 965–975.
[15] C. Salaun, V. Marechal, J.M. Heard, Transport-deficient Pit2 phosphate transporters still modify cell surface oligomers structure in response to inorganic phosphate, J. Mol. Biol. 340 (2004) 39–47.
[16] S. Jono, M.D. McKee, C.E. Murry, A. Shioi, Y. Nishizawa, K. Mori, H. Morii, C.M. Giachelli, Phosphate regulation of vascular smooth muscle cell calcification, Circ. Res. 87 (2000) E10–E17.
[17] C. Wang, Y. Li, L. Shi, J. Ren, M. Patti, T. Wang, J.R. de Oliveira, M.J. Sobrido, B. Quintans, M. Baquero, X. Cui, X.Y. Zhang, L. Wang, H. Xu, J. Wang, J. Yao, X. Dai, J. Liu, L. Zhang, H. Ma, Y. Gao, X. Ma, S. Feng, M. Liu, Q.K. Wang, I.C. Forster, X. Zhang, J.Y. Liu, Mutations in SLC20A2 link familial idiopathic basal ganglia calcification with phosphate homeostasis, Nat. Genet. 44 (2012) 254–256.
[18] M.N. Oda, T.M. Forte, R.O. Ryan, J.C. Voss, The C-terminal domain of apolipoprotein A-I contains a lipid-sensitive conformational trigger, Nat. Struct. Biol. 10 (2003) 455–460.
[19] U. Fristedt, M. van Der Rest, B. Poolman, W.N. Konings, B.L. Persson, Studies of cytochrome c oxidase-driven H+-coupled phosphate transport catalyzed by the *Saccharomyces cerevisiae* Pho84 permease in coreconstituted vesicles, Biochemistry 38 (1999) 16010–16015.
[20] U. Fristedt, R. Weinander, H.S. Martinsson, B.L. Persson, Characterization of purified and unidirectionally reconstituted Pho84 phosphate permease of *Saccharomyces cerevisiae*, FEBS Lett. 458 (1999) 1–5.
[21] J. Petrlova, T. Duong, M.C. Cochran, A. Axelsson, M. Morgelin, L.M. Roberts, J.O. Lagerstedt, The fibrillogenic L178H variant of apolipoprotein A-I forms helical fibrils, J. Lipid Res. 53 (2012) 390–398.
[22] J.A. Morrow, M.L. Segall, S. Lund-Katz, M.C. Phillips, M. Knapp, B. Rupp, K.H. Weisgraber, Differences in stability among the human apolipoprotein E isoforms determined by the amino-terminal domain, Biochemistry 39 (2000) 11657–11666.
[23] G. Kefala, C. Ahn, M. Krupa, L. Esquivies, I. Maslennikov, W. Kwiatkowski, S. Choe, Structures of the OmpF porin crystallized in the presence of foscholine-12, Protein Sci. 19 (2010) 1117–1125.
[24] K. Moncoq, G. Kemp, X. Li, L. Fliegel, H.S. Young, Dimeric structure of human Na+/H+ exchanger isoform 1 overproduced in *Saccharomyces cerevisiae*, J. Biol. Chem. 283 (2008) 4145–4154.

[25] P.M. Hwang, W.Y. Choy, E.I. Lo, L. Chen, J.D. Forman-Kay, C.R. Raetz, G.G. Prive, R.E. Bishop, L.E. Kay, Solution structure and dynamics of the outer membrane enzyme PagP by NMR, Proc. Natl. Acad. Sci. USA 99 (2002) 13560–13565.
[26] R.A. Zvyagilskaya, F. Lundh, D. Samyn, J. Pattison-Granberg, J.M. Mouillon, Y. Popova, J.M. Thevelein, B.L. Persson, Characterization of the Pho89 phosphate transporter by functional hyperexpression in *Saccharomyces cerevisiae*, FEMS Yeast Res. 8 (2008) 685–696.
[27] T. Pourcher, S. Leclercq, G. Brandolin, G. Leblanc, Melibiose permease of *Escherichia coli*: large scale purification and evidence that H+, Na+, and Li+ sugar symport is catalyzed by a single polypeptide, Biochemistry 34 (1995) 4412–4420.
[28] J. Arino, J. Ramos, H. Sychrova, Alkali metal cation transport and homeostasis in yeasts, Microbiol. Mol. Biol. Rev. 74 (2010) 95–120.
[29] J.R. Pratt, J.M. Mouillon, J.O. Lagerstedt, J. Pattison-Granberg, K.I. Lundh, B.L. Persson, Effects of methylphosphonate, a phosphate analogue, on the expression and degradation of the high-affinity phosphate transporter Pho84, in *Saccharomyces cerevisiae*, Biochemistry 43 (2004) 14444–14453.
[30] Y. Popova, P. Thayumanavan, E. Lonati, M. Agrochao, J.M. Thevelein, Transport and signaling through the phosphate-binding site of the yeast Pho84 phosphate transceptor, Proc. Natl. Acad. Sci. USA 107 (2010) 2890–2895.
[31] S.R. Martin, M.J. Schilstra, Circular dichroism and its application to the study of biomolecules, Methods Cell Biol. 84 (2008) 263–293.
[32] L.J. Berliner, J. Grunwald, H.O. Hankovszky, K. Hideg, A novel reversible thiolspecific spin label – papain active site labeling and inhibition, Anal. Biochem. 119 (1982) 450–455.
[33] Z.F. Guo, D. Cascio, K. Hideg, T. Kalai, W.L. Hubbell, Structural determinants of nitroxide motion in spin-labeled proteins: Tertiary contact and solvent-inaccessible sites in helix G of T4 lysozyme, Protein Sci. 16 (2007) 1069–1086.
[34] J.F. Hess, M.S. Budamagunta, A. Aziz, P.G. Fitzgerald, J.C. Voss, Electron paramagnetic resonance analysis of the vimentin tail domain reveals points of order in a largely disordered region and conformational adaptation upon filament assembly, Protein Sci. 22 (2013) 47–55.
[35] L. Columbus, W.L. Hubbell, A new spin on protein dynamics, Trends Biochem. Sci. 27 (2002) 288–295.